JOURNAL OF AGRICULTURAL AND FOOD CHEMISTRY

Kinetic Modeling of 2,4-Dichlorophenoxyacetic Acid (2,4-D) Degradation in Soil Slurry by Anodic Fenton Treatment

LINGJUN KONG AND ANN T. LEMLEY*

Graduate Field of Environmental Toxicology, TXA, MVR Hall, Cornell University, Ithaca, New York 14853-4401

Anodic Fenton treatment (AFT) has been shown to be a promising technology in pesticide wastewater treatment. However, no research has been conducted on the AFT application to contaminated soils. In this study, the 2,4-D degradation kinetics of AFT in a silt loam soil slurry were investigated for the first time, and the effects of various experimental conditions including initial 2,4-D concentration, Fenton reagent delivery rate, amount of humic acid (HA) addition, and pH were examined. The 2,4-D degradation in soil slurry by AFT was found to follow a two-stage kinetic model. During the early stage of AFT (the first 4−5 min), the 2,4-D concentration profile followed a pseudo-first-order kinetic model. In the later stage (typically after 5 or 6 min), the AFT kinetic model provided a better fit. This result is most likely due to the existence of •OH scavengers and 2,4-D sorption on soil. The Fe^{2+} delivery rate was shown to be a more significant factor in degradation rate than the H_2O_2 delivery rate when the Fe^{2+}/H_2O_2 ratios were in the range of 1:2 to 1:10. The presence of HA in soil lowered the AFT rate, most probably due to the competition with 2,4-D for consumption of •OH and increased sorption of 2,4-D on soil. The optimal pH for 2,4-D degradation in soil slurry by AFT was observed to be in the range of pH 2−3.

KEYWORDS: 2,4-D; pesticides; degradation; soil; Fenton reaction; kinetics; hydroxyl radicals; humic acid

INTRODUCTION

Pesticide-contaminated groundwater/soil has been a worldwide problem over the past two decades (*1*−*3*). Because of spills, discharge, or improper disposal during the manufacturing process and/or agricultural activities, pesticides have been generated as industrial wastewater or released into natural environmental systems, causing detrimental ecological and human health consequences. Among various cleanup technologies, advanced oxidation processes (AOPs) have gained increasing attention due to their rapid and complete destruction of target contaminants (*4*, *5*). As one of the most employed and studied AOPs, Fenton/Fenton-like treatment generates hydroxyl radicals (•OH) through decomposition of hydrogen peroxide (H_2O_2) in the presence of catalysts [mainly transition metal catalysts, such as Fe(II), Fe(III), Mn(II) and Mn (IV)]. The classic Fenton reaction can be expressed as

$$Fe^{2+} + H_2O_2 \rightarrow Fe^{3+} + {}^{\bullet}OH + OH^- \quad (1)$$

The generated hydroxyl radical (•OH) is a powerful and nonspecific oxidant, which has been widely accepted as the major intermediate capable of degrading a wide range of organic compounds at a near diffusion-controlled rate (10^9−10^{10} M^{-1} s^{-1}) (*5*−*10*). The principal mechanisms and kinetics of Fenton-like reactions in simple and well-characterized aqueous systems have been consistently well documented (**Table 1**) (*5*, *7*, *8*, *11*−*14*).

Table 1. Summary of Major Chemical Reactions Involved in Fenton-like Treatment

reaction	rate constant, k_i ($M^{-1}s^{-1}$)	ref
$Fe^{2+} + H_2O_2 \rightarrow Fe^{3+} + {}^{\bullet}OH + OH^-$	53–76	*7*
$Fe^{3+} + H_2O_2 \rightarrow Fe^{2+} + {}^{\bullet}O_2^- + OH^-$	2×10^{-3}	*5*
$Fe^{3+} + {}^{\bullet}O_2^- \rightarrow Fe^{2+} + O_2$	3.1×10^5	*8*
$Fe^{2+} + {}^{\bullet}OH \rightarrow Fe^{3+} + OH^-$	$2.3–5 \times 10^8$	*11*
$^{\bullet}OH + H_2O_2 \rightarrow HO_2^{\bullet} + H_2O$	2.7×10^7	*7*
$HO_2^{\bullet} + Fe^{2+} \rightarrow HO_2^- + Fe^{3+}$	1.2×10^6	*7*
$2\,^{\bullet}OH \rightarrow H_2O_2$	5.2×10^9	*11*
$^{\bullet}OH + HCO_3^- \rightarrow CO_3^{2-} + H_2O$	8.5×10^6	*8*
•OH + organics → products	10^8–10^{10}	*5*

In contrast to aqueous systems, soils are complex, heterogeneous, and site-specific media. The existence of ubiquitous minerals, inorganic constituents, soil organic matter (SOM), and microorganisms that can participate in the propagation reactions or trigger other abiotic and biotic processes can significantly affect Fenton-like treatments. For example, iron or manganese oxides and oxyhydroxides, which are widely present in soils, can act as catalysts in the H_2O_2 decomposition reaction (Fenton-like reaction). Some of them could even be more reactive than

* Author to whom correspondence should be addressed [telephone (607) 255-3151; fax (607) 255-1093; e-mail ATL2@cornell.edu].

10.1021/jf060046x CCC: $33.50
Published on Web 04/21/2006

the traditional Fenton reagent (Fe^{2+}) (*5*, *15*−*17*). Bicarbonate (HCO_3^-) and carbonates (CO_3^{2-}), which widely exist in groundwater/subsurface systems, can function as •OH scavengers (*5*, *15*). With respect to the effects of SOM, contradictory results have been reported. SOM is generally accepted as a potential competitive reactant for hydroxyl radicals (•OH), that is, as a •OH scavenger, which has a negative effect on the target compound degradation (*7*, *13*, *15*, *18*, *19*). Organic contaminant sorption in soil due to SOM can also lower the effectiveness of Fenton-like treatments (*10*, *13*, *20*, *21*). On the other hand, humic acid (HA), a complex mixture of decomposed and/or transformed organic materials in soil, was found to play a beneficial role in the Fenton-like process by enhancing the reduction of Fe(III) to Fe(II) (*9*, *22*, *23*). In practice, all of these known or unknown processes may occur and interfere with one another. Due to the complexity, variety, and uncertainty of the soil matrix, the mechanisms and reaction kinetics of Fenton-like processes in soil have not been well understood, which hinders the application and improvement of remediation technologies.

For soil and groundwater contamination, many research and industrial efforts using AOPs can be characterized as in situ chemical oxidation (ISCO), that is, treatment in the place of the contamination (*21*, *24*−*26*). ISCO-based technologies have the advantage of lowering the operating cost and making full use of the naturally existing oxidants or catalysts while effectively destroying target contaminants. However, ISCO is significantly influenced by the hydrological, physical−chemical, and microbial conditions of the aquifer. On the other hand, ex situ chemical oxidation (ESCO) can be more expensive due to the cost of removing soil from the contaminated site; nevertheless, it can provide a more controlled operating condition and result in higher contaminant removal efficiency.

Anodic Fenton treatment (AFT) is an indirect electrochemical treatment used to degrade pesticides by generating Fe^{2+} via electrolysis, as shown in eqs 2 and 3:

$$\text{anode: } Fe \rightarrow Fe^{2+} + 2e^2 \quad (2)$$

$$\text{cathode: } 2H_2O + 2e \rightarrow H_2 + 2OH^- \quad (3)$$

AFT is reported to be capable of removing >99% of many pesticides, such as 2,4-dichlorophenoxyacetic acid (2,4-D), carbaryl, carbamate, carbofuran, and metribuzin, from aqueous systems within 10 min (*27*−*30*). The AFT kinetic model has been developed to simulate pesticide degradation in aqueous systems, and it provides a very good fit to the concentration profiles of pesticides during the AFT process in most cases (*27*−*29*). AFT has shown a great potential in pesticide wastewater treatment as an effective cleanup technology, but no research has been performed to apply the AFT to soil/water systems.

The purpose of this research is to apply AFT to the treatment of pesticide-contaminated soils in an effort to seek an effective ex situ soil remediation technology. The kinetic modeling investigations are expected to provide a fundamental perspective and quantitative tool to optimize the treatment conditions. The specific objectives of this research are (1) to investigate the kinetics of 2,4-D degradation in soil slurry by AFT; (2) to examine the effects of various experimental conditions such as initial 2,4-D concentration, Fenton reagent delivery rate, Fe^{2+}/H_2O_2 delivery ratio, HA content, and initial pH on 2,4-D degradation kinetics; and (3) to develop correlations between various experimental conditions and reaction rate constants and/or Fe^{2+}/•OH lifetimes to provide quantitative tools for the optimization of AFT conditions.

Table 2. Relevant Properties of Field Soil Used in This Study

pH	moisture (%)	organic C (wt %)	clay (wt %)	silt (wt %)	sand (wt %)	CEC (mmol/kg)
6.75	3.79	2.54	28.42	51.84	29.74	177.4

MATERIALS AND METHODS

Chemicals. 2,4-D (98%), hydrogen peroxide (30%), and humic acid (48.95% OC) were purchased from Sigma-Aldrich Chemicals (Milwaukee, WI). Acetonitrile (HPLC grade), methanol, phosphoric acid (85%), sodium chloride, and water (HPLC grade) were purchased from Fisher Scientific (Fair Lawn, NJ). Sulfuric acid (95.4%) was purchased from Mallinckrodt (Paris, KY). All reagents used were of certified grade except where specifically indicated. Deionized (DI) water was obtained from a Barnstead Nanopure system with an electric resistance of effluent water >18.1 MΩ cm^{-1}. All solutions were prepared from DI water.

Solid Matrix. White quartz sand (50 + 70 mesh) (designated sand) was purchased from Sigma-Aldrich Chemicals and used as purchased. The field soil (designated soil) was collected at 0−20 cm depth from a farm field at Cornell University in Ithaca, NY. Prior to use, the soil was air-dried at room temperature (22.0 ± 1.0 °C) and then gently ground to pass through a 2 mm sieve. Relevant soil properties are summarized in **Table 2**. On the basis of the texture result, this soil is classified as a silt loam soil.

Degradation of 2,4-D in Soil Slurry by AFT. The AFT apparatus consisted of two 250 mL customized glass half-cells (anodic and cathodic half-cells) separated by an anion exchange membrane (Electrosynthesis, Lancaster, NY) with an electric resistance of 8 Ω cm^{-2} in 1 M NaCl. A pure iron plate (2 cm × 10 cm × 0.2 cm) and a graphite rod [1 cm (i.d.) × 10 cm (length)] were used as anode and cathode, respectively. The electric current (*I*) was supplied by a BK Precision DC power supply 1610. Approximately 200 mL of 2,4-D solution or contaminated sand/soil slurry with a NaCl concentration of 0.02 M and the same volume of 0.08 M NaCl solution were added to the anodic and cathodic half-cells, respectively. For aqueous and sand/water systems, no pH adjustment was conducted. For soil slurry, the pH was adjusted to 3.0 using sulfuric acid prior to AFT. The soil slurry or solution in each half-cell was mixed by a magnetic stirring bar during the AFT process. Soil slurries were prepared by adding soil to the 2,4-D solution to obtain a soil/solution ratio of 1:5 and then allowing them to reach equilibrium on an Innova 2300 Platform shaker (New Brunswick Scientific, Edison, NY) with a shaking speed of 200 rpm for 24 h. Hydrogen peroxide was delivered into the anodic half-cell using a Stepdos peristaltic pump (Chemglass Inc., Vineland, NJ) at a

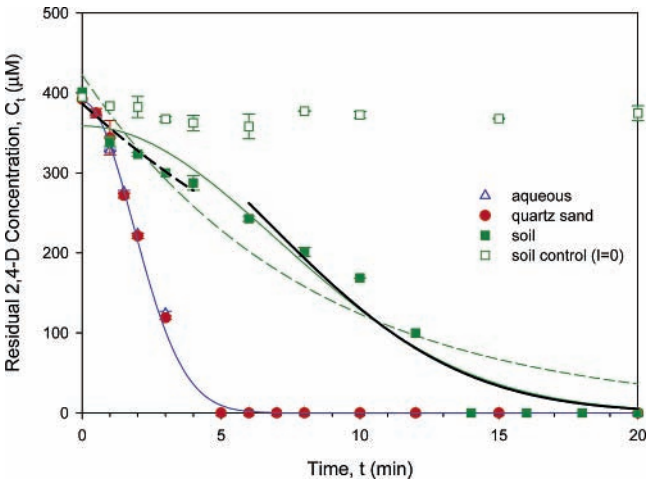

Figure 1. Comparison of 2,4-D degradation kinetics in aqueous, quartz sand/water, and soil/water systems with initial 2,4-D concentration of 400 μM. Dashed lines represent pseudo-first-order kinetic model fit, and solid lines represent AFT kinetic model fit.

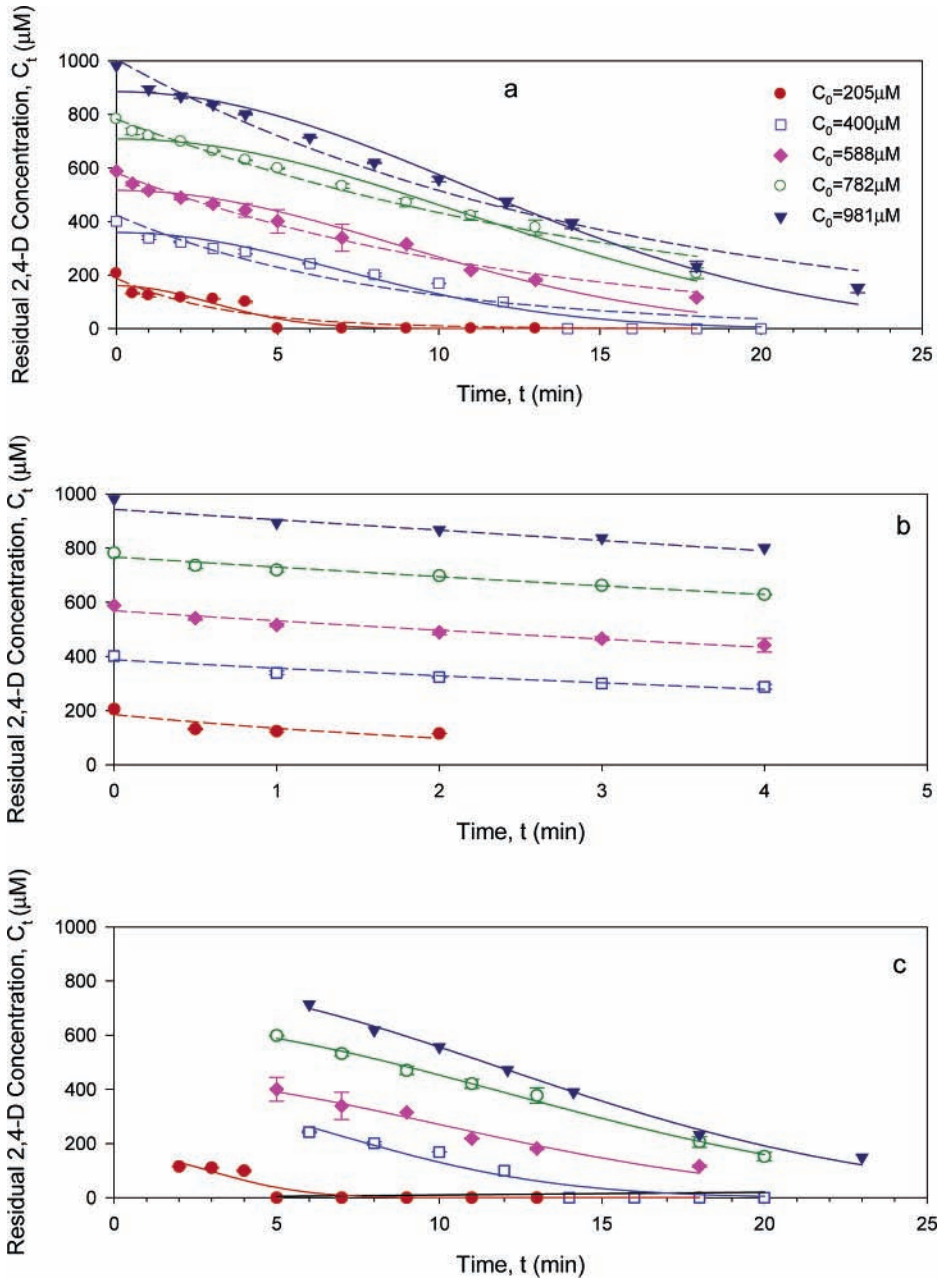

Figure 2. Kinetic modeling of 2,4-D degradation in soil slurry at different initial concentrations: (**a**) pseudo-first order and AFT kinetic model fit; (**b**) pseudo-first order kinetic model fit in early stage; (**c**) AFT kinetic model fit in later stage. Dashed lines represent pseudo-first-order kinetic model fit, and solid lines represent AFT kinetic model fit.

flow rate of 0.50 mL min^{-1}. Unless specified otherwise, electric current was kept at 0.050 A, and the corresponding H_2O_2 concentration was 0.223 M, which resulted in a Fe^{2+}/H_2O_2 delivery ratio of 1:7.2. The DC power supply was turned on, and the electric current was adjusted to a certain value once the first drop of hydrogen peroxide entered the soil slurry in the anodic half-cell. Over a time period of 20 min, 0.6 mL of soil slurry was taken out at certain time intervals and transferred to a 1.5 mL centrifuge tube containing 0.6 mL of methanol, which served as both quencher of hydroxyl radicals and extractor of 2,4-D from soil. The mass recovery of 2,4-D after methanol extraction was determined to be >95%. The collected soil slurries were then mixed vigorously on a Thermodyne Type 16700 touch mixer (Dubuque, IA) for 1 min to extract the 2,4-D sorbed on soil. The soil slurries were then centrifuged at 10000 rpm for 10 min using an Eppendorf minispinner (Germany). The supernatant was collected in a 2 mL GC vial for 2,4-D concentration analysis. All experiments were performed at room temperature (22.0 ± 1.0 °C). Each treatment was repeated twice.

Concentration Analysis of 2,4-D and Hydrogen Peroxide. The 2,4-D concentration was analyzed by a reverse-phase high-performance liquid chromatography (HPLC) system equipped with a Restek ultra C18 (5 μm) column (4.6 × 150 mm) and a diode array (DAD) UV−vis detector (HP series 1100, Agilent Technology). The DAD wavelength was chosen at 280 ± 20 mm. The mobile phase consisted of acetonitrile and water with an acetonitrile/water ratio of 60:40. The pH of the water phase was adjusted to 3.0 using phosphoric acid. The retention time of 2,4-D under the described analytical conditions was 5.01 min. The average recovery of 2,4-D by HPLC analysis under the described conditions was 98.9%, and the method detection limit (MDL) was 0.041 μM at the 99% confidence interval.

The concentration of hydrogen peroxide was determined by potassium permanganate titration (*31*).

Experimental Data Analysis. All of the figures and statistical analyses [except analysis of variance (ANOVA)] were completed using SigmaPlot 9.0 (*32*). ANOVA was performed using Minitab 14 (*33*).

Table 3. Two-Stage Kinetic Modeling of 2,4-D Degradation in Soil Slurry at Different Initial 2,4-D Concentrations

initial concn, C_0 (μM)	pseudo-first-order model (early stage)	AFT model (later stage)
205	$\ln(C_t/C_0) = -(0.320 \pm 0.148)t$ $r^2 = 0.71$	$\ln(C_t/C_0) = -(0.0590 \pm 0.0203)t^2$ $r^2 = 0.81$
400	$\ln(C_t/C_0) = -(0.0830 \pm 0.0138)t$ $r^2 = 0.92$	$\ln(C_t/C_0) = -(0.0141 \pm 0.0038)t^2$ $r^2 = 0.86$
588	$\ln(C_t/C_0) = -(0.0677 \pm 0.0084)t$ $r^2 = 0.94$	$\ln(C_t/C_0) = -(4.89 \pm 0.59) \times 10^{-3}t^2$ $r^2 = 0.97$
782	$\ln(C_t/C_0) = -(0.0499 \pm 0.0047)t$ $r^2 = 0.97$	$\ln(C_t/C_0) = -(3.48 \pm 0.15) \times 10^{-3}t^2$ $r^2 = 0.99$
981	$\ln(C_t/C_0) = -(0.0695 \pm 0.0044)t$ $r^2 = 0.97$	$\ln(C_t/C_0) = -(3.56 \pm 0.17) \times 10^{-3}t^2$ $r^2 = 0.99$

RESULTS AND DISCUSSION

Comparison of 2,4-D Degradation Kinetics in Soil Slurry and Aqueous Solution. The degradation of organic compounds by •OH is typically described as a second-order reaction (*5*, *7*)

$$-\frac{dC}{dt} = kC[^{\bullet}OH] \quad (4)$$

where C and [•OH] are concentrations of the target organic compound and •OH, respectively, k is the second-order rate constant, and t is the reaction time.

According to the previously developed AFT kinetic model, 2,4-D residual concentration at treatment time t (C_t) in aqueous solution can be expressed as (*27*)

$$\ln\frac{C_t}{C_0} = -\frac{1}{2}K\lambda\pi\omega{v_0}^2t^2 \quad (5)$$

where C_0 is the 2,4-D initial concentration ($t = 0$) (μM), $K = kk_1$, and k and k_1 are the second-order rate constants of the reaction between 2,4-D and •OH and the Fenton reaction (μM^{-1} min^{-1}), respectively; λ and π are the average lifetimes of •OH and Fe^{2+} (min), respectively, ω is a constant related to Fe^{2+}/H_2O_2 delivery ratio, and v_0 is the Fe^{2+} delivery rate (μM min^{-1}). The "lumped" parameter $K\lambda\pi\omega{v_0}^2$ is referred to as the AFT rate constant (min^{-2}). The AFT kinetic model assumes that the instantaneous •OH concentration is proportional to the •OH generation rate, which is assumed to increase linearly with reaction time (t).

Another widely accepted kinetic model of degradation of organic compounds by Fenton-like treatment is the pseudo-first-order model as shown in eq 6, which assumes that •OH instantaneous concentration is constant (*7*, *19*)

$$\ln\frac{C_t}{C_0} = -k_{app}t \quad (6)$$

where k_{app} is the first-order apparent rate constant (min^{-1}).

From the observed 2,4-D concentration profiles (**Figure 1**), there is no significant difference between the results obtained in the aqueous system and the sand/water system (ANOVA confidence level 95%, $P = 1.00$). The 2,4-D concentration in the anodic cell was below the detection limit within 5 min in both systems, whereas the 2,4-D degradation rate in soil slurry was much slower than that in aqueous solution and quartz sand slurry, and 2,4-D was not detected after 15 min of treatment. Quartz sand used in this experiment is a uniform sand with no organic carbon detected. Thus, the sorption of 2,4-D in this sand is negligible, and no additional •OH scavengers, other than those in the corresponding aqueous system, exist. However, the field soil slurry is a much more complicated matrix. Both 2,4-D sorption/desorption and exotic •OH scavengers (i.e., SOM) could greatly affect the 2,4-D degradation rate. According to the sorption isotherm (data not shown), 2,4-D sorption in the soil is <7.2% with a soil/solution ratio of 1:5 at room temperature, indicating that sorption should not significantly affect the 2,4-D degradation in soil slurry. The discrepancy of the 2,4-D concentration profiles in the three systems examined should be mainly caused by the existence of a large amount of potential •OH scavengers in the soil, such as SOM. Lindsey and Tarr (*18*, *34*) have observed that the presence of natural organic matter (NOM) can inhibit the target compound degradation by •OH. The Fe^{2+} could also exchange on soil, potentially lowering its ability to participate in the AFT process. However, considering the continuous delivery of Fe^{2+} in the AFT, the effect of the exchange of Fe^{2+} should not be as critical as that of •OH scavengers.

Quantitatively, the AFT kinetic model provided a very good simulation of the experimental data in aqueous solution and quartz sand slurry ($r^2 = 1.00$). However, neither the AFT nor the pseudo-first-order model could fit very well the 2,4-D concentration profile in soil slurry over the entire evaluated treatment time period (0−20 min). Visually, the AFT model could not fit the data in the early stage of the treatment (0−5 min), which is better described as an exponential decrease. In the later stage of 2,4-D degradation (after 5 min), the AFT kinetic model provided a better fit, whereas the pseudo-first-order model showed a much longer tailing. On the basis of the above observations, a two-stage kinetic model of the 2,4-D degradation in soil slurry was proposed. That is, the 2,4-D concentration profile was considered to follow the pseudo-first-order kinetic model in the early stage of AFT treatment and then transition to the AFT model in the later stage. The reason for the kinetics transition during the treatment process could

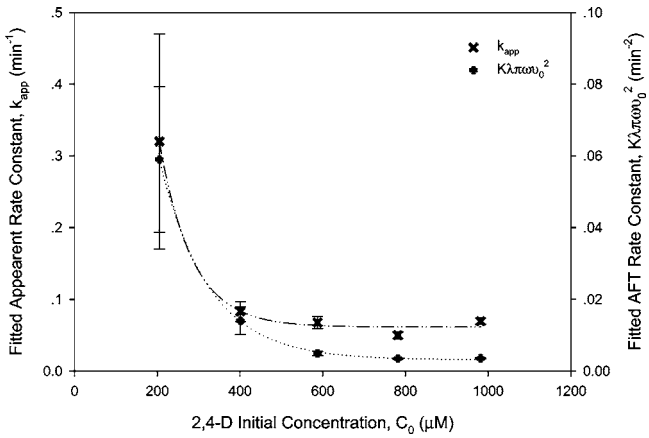

Figure 3. Correlations between fitted rate constants (k_{app} and $K\lambda\pi\omega{v_0}^2$) and 2,4-D initial concentrations. Dotted line represents fitted values, and dashed/dotted line represents regression lines.

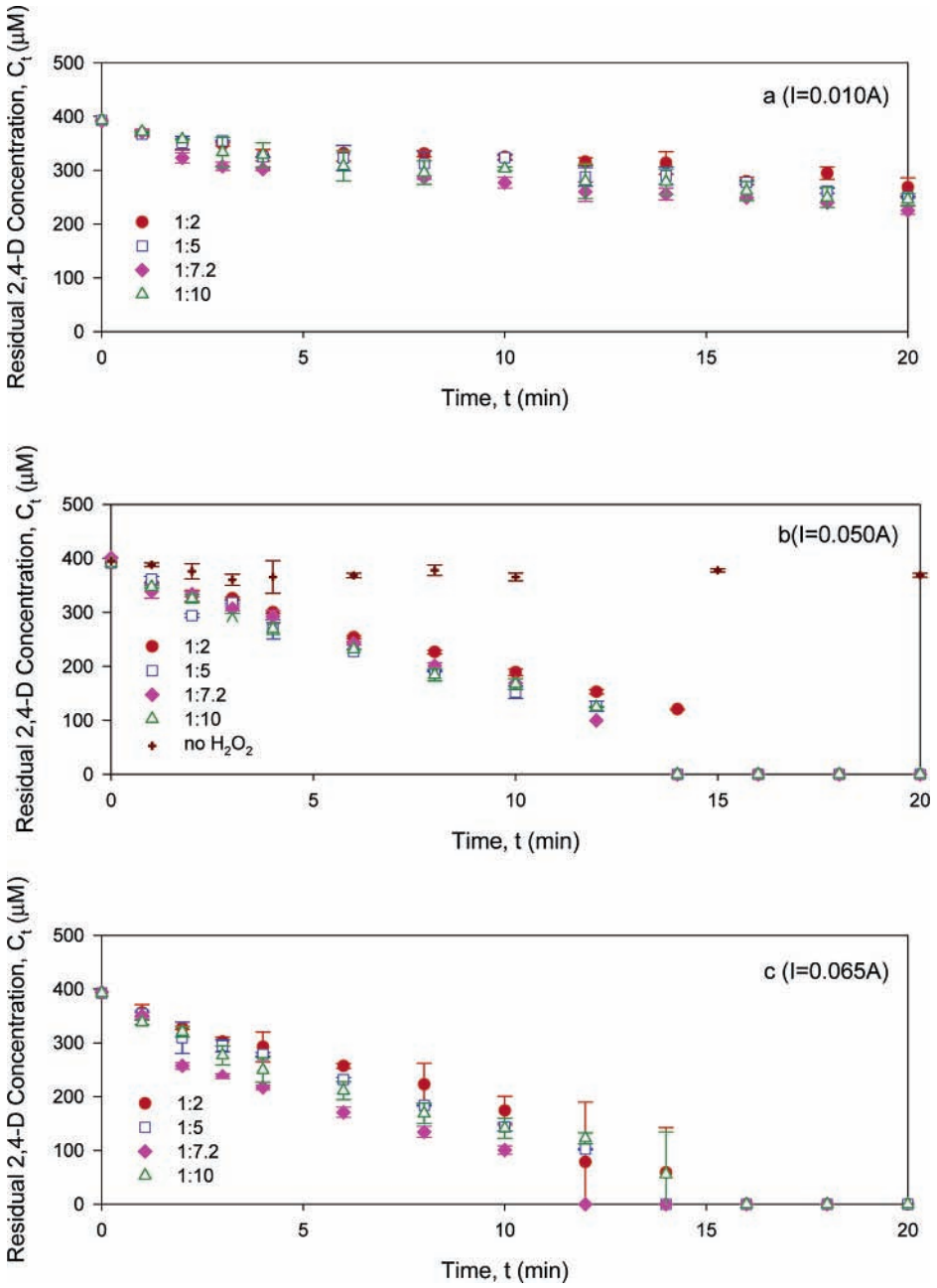

Figure 4. Effect of Fe^{2+} delivery rate and Fe^{2+}/H_2O_2 ratio on degradation rate of 2,4-D: (**a**) $I = 0.010A$; (**b**) $I = 0.050A$; (**c**) $I = 0.065A$.

be attributed to the existence of a large amount of •OH scavengers in the field soil and 2,4-D sorption on soil. During the early stage of AFT, the •OH scavengers in soil, such as SOM, could react with •OH and consume a significant part of the generated •OH, which would probably keep the instantaneous •OH concentration in the system invariant and result in pseudo-first-order kinetics. The sorption of 2,4-D might also contribute to the relatively slow degradation rate of 2,4-D in the soil slurry compared to the aqueous solution, especially in the early stage, which is reflected in the pseudo-first-order kinetics and is similar to what is observed in other organic compound degradation in soil slurries (*7*). As the Fenton-like reaction proceeds, •OH scavengers most probably decrease dramatically, resulting in a system more similar to the aqueous or quartz sand slurry, which would fit the AFT kinetic model. Wang and Lemley (*19*) also observed a kinetics transition from AFT to a pseudo-first-order model as the amount of HA in alachlor solution increased. As the residual 2,4-D concentration in the system becomes very low (close to complete degradation), the AFT kinetics do not fit the experimental data very well; that is, the observed 2,4-D concentration exhibits a "sudden" drop to below the detection limit. This most likely results from the possible sorption of 2,4-D on soil even after methanol extraction.

Effect of Initial 2,4-D Concentration on 2,4-D Degradation Kinetics. 2,4-D degradation in soil slurry was investigated at five initial concentration levels (205, 400, 588, 782, and 981 μM) as shown in **Figure 2a**. All of the 2,4-D concentration profiles were fitted with both the pseudo-first-order and AFT kinetic models, respectively. As pointed out in the above section, neither of the two models fitted the experimental data very well independently. The pseudo-first-order model could not satisfy the later stage, and the AFT model did not fit the early stage. When the two-stage kinetic model was employed, that is, the pseudo-first-order and AFT models were used to fit the concentration profile during the first 4 min and after 5 min, respectively, a fairly good simulation of the concentration

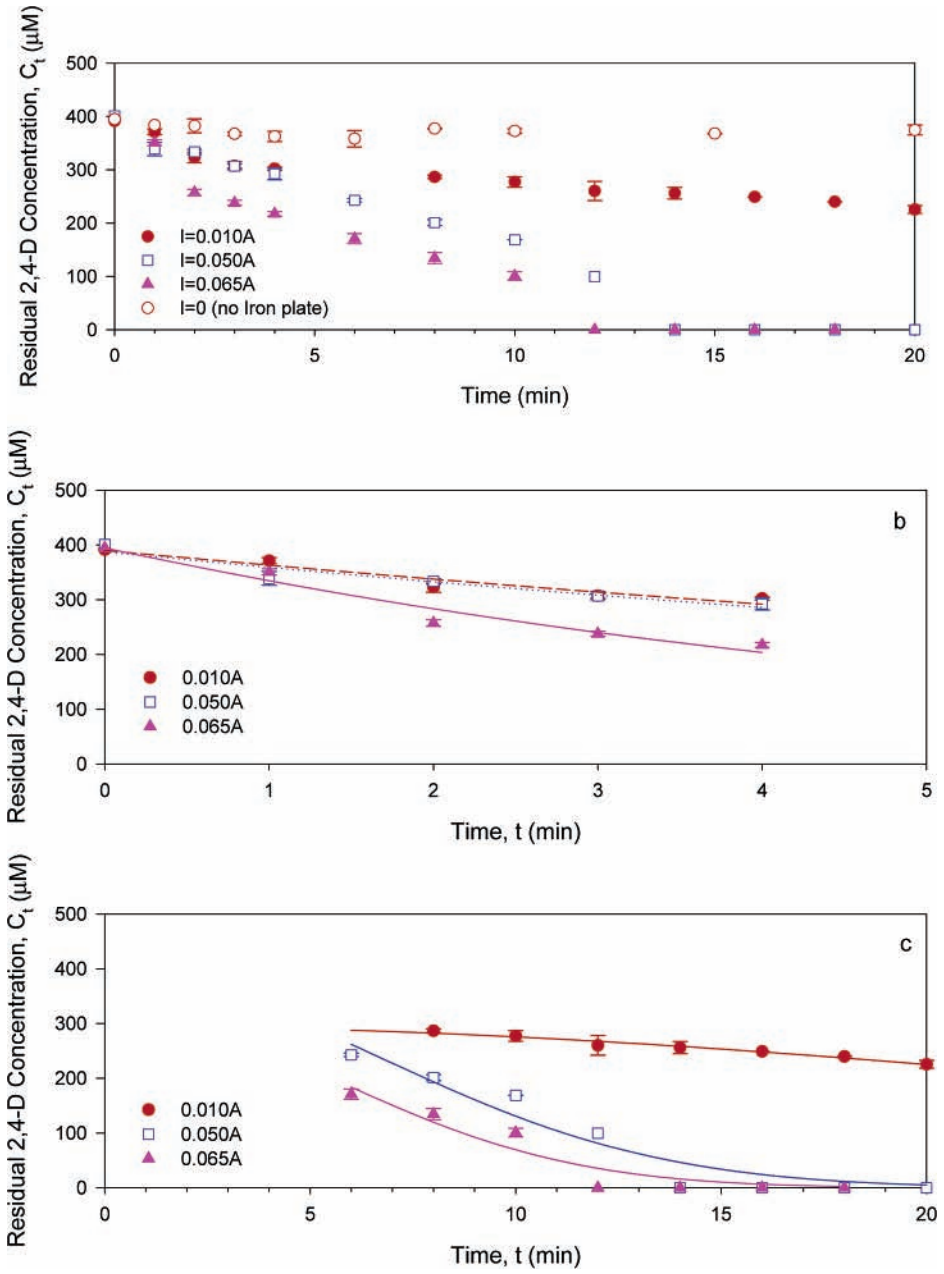

Figure 5. Effect of Fe^{2+} delivery rate on 2,4-D degradation kinetics (Fe^{2+}/H_2O_2 = 1:7.2): (**a**) 2,4-D concentration profiles; (**b**) pseudo-first-order kinetic model fit in early stage; (**c**) AFT kinetic model fit in later stage. Dashed lines represent pseudo-first-order kinetic model fit, and solid lines represent AFT kinetic model fit.

profiles was obtained as shown in **Figure 2b,c** and **Table 3**. In the case of the lowest evaluated concentration (i.e., C_0 = 205 μM), the kinetics transition region shifted to an earlier time (≈2 min), most likely because the degradation process was completed in 5 min. The relatively lower r^2 value can be explained by the fact that there were not enough data points during this period of time to obtain a better regression. On the basis of the two-stage kinetic model, the degradation rate constants (k_{app} and $K\lambda\pi\omega v_0^2$) exhibited an exponential decrease with increasing 2,4-D initial concentration (**Figure 3**). In other words, 2,4-D degraded more rapidly at low concentration than at high concentration. When the initial concentration reached a certain level (≈400 μM under the evaluated experimental conditions), the 2,4-D degradation rate hardly changed with increasing initial concentration. Because K is the product of two reaction rate constants, and ω and v_0 were fixed, the differences among AFT rate constants ($K\lambda\pi\omega v_0^2$) at each initial 2,4-D concentration were caused by a change in the lifetimes of Fe^{2+} and $^{\bullet}OH$, which were related to λ and π, respectively. Therefore, the fact that the rate constant decreased exponentially with increasing initial concentration implies an exponential decrease of $Fe^{2+}/^{\bullet}OH$ lifetimes with increasing initial concentration; that is, the higher the initial concentration, the faster Fe^{2+} and $^{\bullet}OH$ are consumed. A similar trend of rate constant and $Fe^{2+}/^{\bullet}OH$ lifetimes as a function of treatment time was found in our laboratory during 2,4-D degradation with different initial concentrations in an AFT aqueous system (*27*).

Effect of Delivery Rate of Fenton Reagents and Fe^{2+}/H_2O_2 Ratio on 2,4-D Degradation Rate. To investigate the effect of delivery rate of Fenton reagent (Fe^{2+} and H_2O_2) and Fe^{2+}/H_2O_2 delivery ratio on 2,4-D degradation kinetics, three current levels (0.010. 0.050, and 0.065 A, corresponding to Fe^{2+} delivery rates of 15.6, 77.7, and 101.4 μM min^{-1}, respectively) were applied. At each current level H_2O_2 concentration was

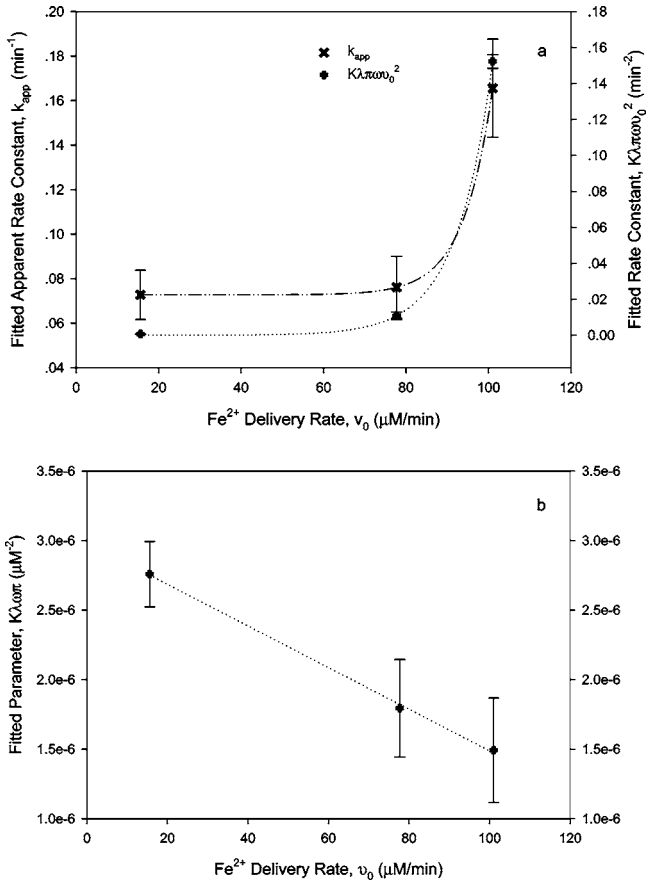

Figure 6. Correlations between (**a**) fitted rate constants (k_{app} and $K\lambda\pi\omega v_0^2$) and Fe^{2+} delivery rates and (**b**) $K\lambda\pi\omega$ and Fe^{2+} delivery rate.

adjusted to achieve four Fe^{2+}/H_2O_2 delivery ratios (1:2, 1:5, 1:7.2, and 1:10). The observed 2,4-D concentration profiles (**Figure 4**) showed no significant difference among the cases with different Fe^{2+}/H_2O_2 ratios at each current level at a confidence level of 95% ($P > 0.99$) by ANOVA. Considering that H_2O_2 is involved in both productive and nonproductive reactions with respect to yielding •OH, the excessive amount of H_2O_2 does not necessarily result in the generation of •OH. (*5*, *7*, *27*). However, under different current levels or different Fe^{2+} delivery rates but identical Fe^{2+}/H_2O_2 delivery ratios, the degradation rate increased with increasing current value or Fe^{2+} delivery rates. On the basis of the control experimental ($I = 0$) (**Figure 5a**), the 2,4-D concentration in the anodic cell showed little change in the course of 20 min, indicating that the effect of iron species in the soil could be neglected. At low current/Fe^{2+} delivery rate (0.010 A/15.6 μM min^{-1}), the removal of 2,4-D from soil slurry was <40%; when the current was >0.050A (or the Fe^{2+} delivery rate was >77.7 μM min^{-1}), 2,4-D was degraded to below the detection limit within 15 min. This observation implies that the delivery rate of Fe^{2+} in the range of 15.6−101.4 μM min^{-1} is a more significant factor in the 2,4-D degradation rate than the H_2O_2 delivery rate when the Fe^{2+}/H_2O_2 ratios are in the range of 1:2 to 1:10. To better compare the degradation rates of 2,4-D at various currents or Fe^{2+} delivery rates, the data with the same Fe^{2+}/H_2O_2 delivery ratio of 1:7.2 and different currents (0.010, 0.050, and 0.065A) were selected and plotted in a separate figure (**Figure 5a**). The 2,4-D degradation at a current of 0.010 A is obviously slower than those at 0.050 and 0.065 A. One thing in common is that the 2,4-D concentration profiles at the three current values followed the previously proposed two-stage kinetic model as shown in **Figure 5b**,**c**. With respect to the fitted rate constants (k_{app} and $K\lambda\pi\omega v_0^2$) (**Figure 6a**), when the Fe^{2+} delivery rate was <80 μM min^{-1} ($I < 0.050$A), no apparent change of the rate constants was observed; when the Fe^{2+} delivery rate was >80 μM min^{-1} ($I > 0.050$A), the rate constants displayed a dramatic increase. As shown in **Figure 6b**, the "lumped" parameter $K\lambda\pi\omega$ decreased with increasing Fe^{2+} delivery rate, indicating the lifetimes of Fe^{2+}/•OH decreased with increasing Fe^{2+} delivery rates, which implies a higher degradation rate at higher Fe^{2+} delivery rate. These observations were consistent with the 2,4-D degradation rate in the aqueous phase under different Fenton reagent delivery rate (*27*).

Effect of the Amount of HA Addition on 2,4-D Degradation Kinetics. To investigate the effect of HA content, field soil was amended with HA in the amounts of 0, 0.5, 1.0, and 5.0% (wt). The 2,4-D residual concentrations in soil slurries with different amounts of HA are plotted as a function of treatment time (**Figure 7a**). It is interesting to note that when the HA addition is as high as 5%, the pseudo-first-order kinetic model provides a good fit to the experimental data over the entire time period (1−20 min) ($r^2 = 0.97$), whereas a two-stage kinetic model is needed to better satisfy the 2,4-D concentration profiles in three other cases with HA additions of 0, 0.5, and 1.0%. As discussed in the previous section, the existence of large amounts of •OH scavengers and 2,4-D sorption on soil were responsible for the kinetic discrepancy. When the HA addition was as high as 5%, the •OH scavenger content would remain at a high level for the entire treatment process (20 min), which would be reflected in a constant •OH instantaneous concentration and would result in pseudo-first-order degradation kinetics. In addition, the increase of 2,4-D sorption to soil due to the amendment of HA could lower the degradation rate. The sorption values of 2,4-D to soil with HA amendments of 0, 0.5, 1.0, and 5% were determined to be 7.2, 7.7, 8.8, and 11.4%, respectively. Because the sorption/desorption is a much slower process than the AFT degradation, the increased sorption of 2,4-D could result in a slower degradation, that is, a gradual leveling-off of the concentration versus time curve, which is more like pseudo-first-order than AFT kinetics with increased HA addition. When the HA added was up to 5%, the 2,4-D degradation showed an exponential decrease with treatment time. Under this circumstance, the removal of 2,4-D from soil slurry is ≈61% after 20 min due to the competition for •OH between HA and 2,4-D as well as 2,4-D sorption to soil and HA. In contrast, 2,4-D was not detected within 20 min without HA addition or with an HA addition of 0.5 and 1.0%. During the first 4 min there is no significant difference among the acquired data with HA addition of 0, 0.5, and 1.0% (wt) at a confidence level of 95% by ANOVA (**Figure 7b**). Within this time course, the 2,4-D concentration profile was fitted to the pseudo-first-order model, and a satisfactory fit was obtained ($r^2 = 0.94$). In the later stage (after 6 min), experimental data in the case of 0 and 0.5% HA addition presented no significant difference at a confidence level of 95% (AFT rate constant $K\lambda\pi\omega v_0^2 = 0.0098 \pm 0.0014$ min^{-2}), whereas 2,4-D degraded slightly more slowly in the soil slurry with the HA addition of 1.0% ($K\lambda\pi\omega v_0^2 = 0.0052 \pm 0.0012$ min^{-2}). The AFT kinetic model did provide a fairly good fit for the 2,4-D concentration profiles during this period of time (after 6 min, **Figure 7c**) with r^2 values of 0.93 and 0.87 for 0.0 and 0.5% and 0.87 for 1.0%.

Effect of pH on 2,4-D Degradation Kinetics. The optimal pH for the Fenton reaction is typically in the range of pH 2−3 (*35*). In aqueous systems the pH can drop to <3.0 right after

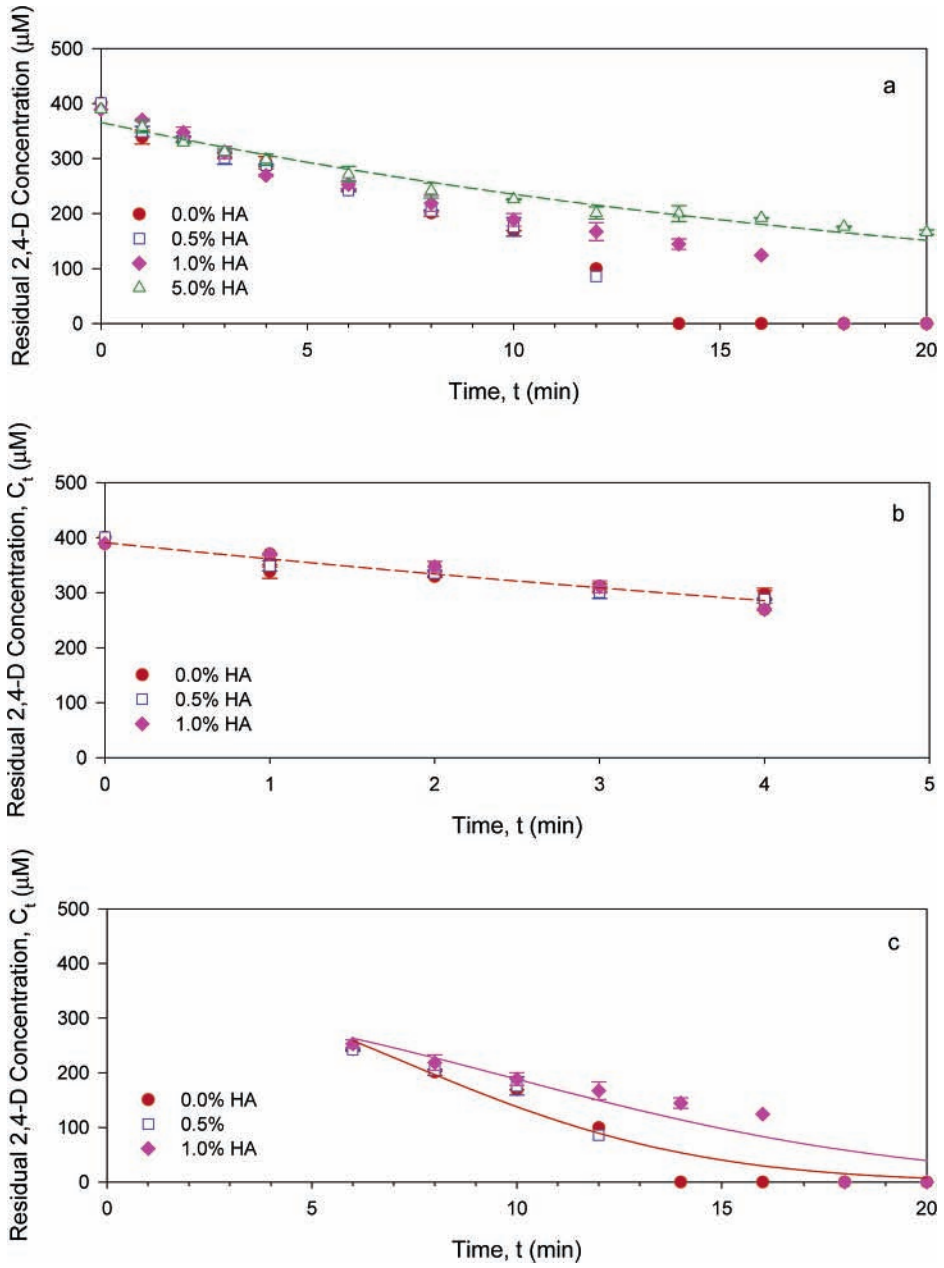

Figure 7. Effect of HA additions to soil on 2,4-D degradation kinetics: (**a**) 2,4-D concentration profiles (dashed line is the pseudo-first-order fit to the case of 5% HA addition); (**b**) pseudo-first-order kinetic model fit in early stage (0, 0.5, and 1.0% HA addition); (**c**) AFT kinetic model fit in later stage (0, 0.5, and 1.0% HA addition).

the Fenton reaction begins, due to the Fenton reagent and Fenton reaction characteristics. The low pH prevents iron species from precipitating and also helps to form a more reduced condition, which benefits the Fenton reaction (*5*). In the soil slurry system, the pH decreases slightly during the Fenton-like treatment due to the strong soil buffer capacity. To test the effect of pH in this system, a series of experiments was conducted at varied pH (pH 2.0, 3.0, 4.0, and 6.7). The results are shown in **Figure 8a**. The initial pH of soil slurry was ≈6.6−6.7 without sulfuric acid addition. After 2 h of AFT performance, the pH dropped to ≈5.6. Less than 30% of 2,4-D was degraded within 20 min, and the residual 2,4-D was still as high as 36% even after 2 h of treatment. As shown in the figure, the 2,4-D degradation rate increased with decreasing initial pH values. In addition, at pH 4.0 and 6.7, the 2,4-D residual concentration in soil slurry exhibited an exponential decrease with time (pseudo-first-order kinetics) over the entire treatment period (20 min). At pH 3.0 and 2.0, a two-stage kinetics was observed, and the kinetics transition region shifted to an earlier time region as the slurry became more acidic. For instance, at pH 2.0, the exponential decrease occurred during the first 2 min, and the rest of the data (after 2 min) followed the AFT model, whereas the kinetics transition happened at ≈4−5 min at pH 3.0. Similar to the results with HA addition, the effect of pH on 2,4-D degradation kinetics showed a kinetics transition from pseudo-first-order to a two-stage kinetic model over the evaluated time period, and the transition region shifted to an earlier time region as the pH dropped. In the case of HA, •OH scavengers and 2,4-D sorption to soil and HA are suggested to be responsible for the transition. With respect to pH, the deactivation of the Fenton reagent (i.e., iron species) caused by precipitation at high pH could slow the generation rate of •OH. Another advantage of low pH is the minimization of the •OH scavenging by HCO_3^- and CO_3^{2-}, which would be more likely to be released as CO_2 at pH 2−3 (pK_a = 4.5) (*5*). As shown in **Figure 8b**, the fitted apparent rate constant decreased with increasing pH: the rate constant

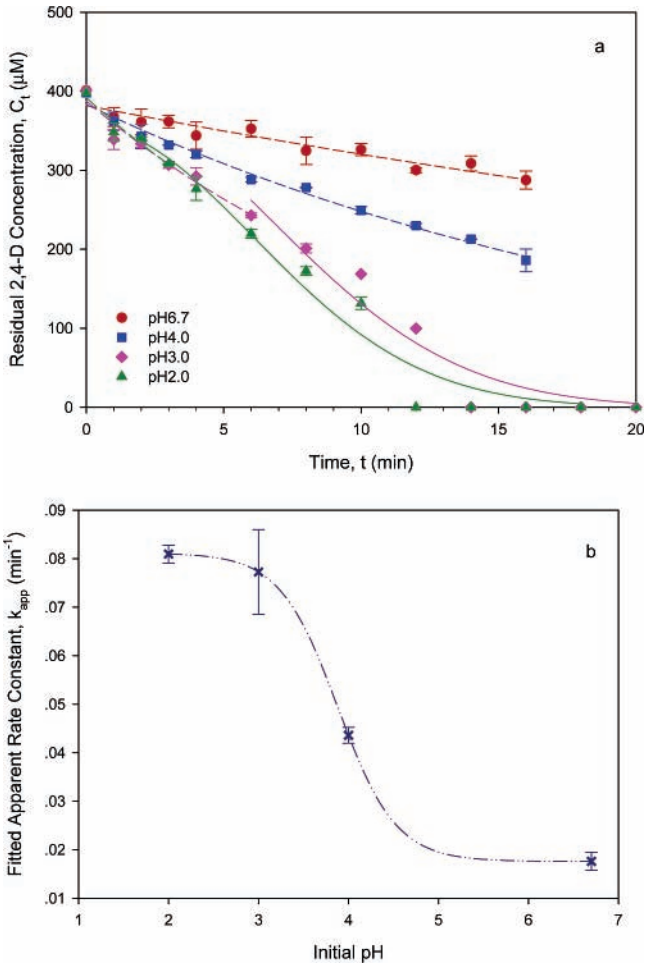

Figure 8. Effect of initial pH values on 2,4-D degradation kinetics: (**a**) concentration profiles at pH 2.0, 3.0, 4.0, and 6.7; (**b**) correlations between fitted apparent rate constant (k_{app}) and initial pH. Dashed lines represent pseudo-first-order kinetic model fit, and solid lines represent AFT kinetic model fit.

decreased dramatically over the pH range of 3−5, and when the pH was <3 or >5, the rate constant showed little change with pH. This observation implies that the optimal pH of 2,4-D degradation in soil slurry by AFT is consistent with the optimal pH of the Fenton reaction in the aqueous phase, which is in the range of pH 2−3. Therefore, in natural groundwater/subsurface systems with a pH value typically in the range of 6−7, a pH adjustment is recommended prior to the AFT to achieve an effective contaminant degradation.

Conclusions and Implications. Although this research is in its initial stages of development, AFT has been shown to be a potentially effective ex situ remediation technology for relatively small-scale pesticide-contaminated sites. The 2,4-D degradation rate increased with decreasing initial concentration and Fe^{2+} delivery rate. The Fe^{2+} delivery rate was shown to be a more significant factor than H_2O_2 when the Fe^{2+}/H_2O_2 delivery ratio was in the range of 1:2 to 1:10. High organic matter content in soil lowers the AFT effectiveness due to the competition for $^{\bullet}OH$ between soil organic matter and target contaminants, as well as pesticide sorption on soil. Therefore, to apply the AFT to a pilot- or full-scale level, characterization of the contaminated sites is critical, that is, the approximate amount of pesticide spilled or discharged, the SOM and mineral contents, etc. The optimal pH for 2,4-D degradation by AFT is in the range of pH 2−3, which implies that a pH adjustment prior to soil slurry treatment by AFT would yield a more effective result due to the strong buffer capacity of field soils. In practice, the soil slurry in the anodic half-cell could be mixed with the cathodic solution after the AFT to partially neutralize the acidic condition of the soil slurry, and the pH could be further adjusted with a basic solution if necessary.

ACKNOWLEDGMENT

We are grateful to Dr. Qiquan Wang for providing soil and soil property data.

LITERATURE CITED

(1) Felsot, A. S.; Racke, K. D.; Hamilton, D. J. Disposal and degradation of pesticide waste. *Rev. Environ. Contam. Toxicol.* **2003**, *177*, 123−200.

(2) Kolpin, D. W.; Thurman, E. M.; Goolsby, D. A. Occurrence of selected pesticides and their metabolites in near-surface aquifers of the midwestern United States. *Environ. Sci. Technol.* **1996**, *30* (5), 335−340.

(3) Thurman, E. M.; Goolsby, D. A.; Meyer, M. T.; Mills, M. S.; Pomes, M. L.; Kolpin, D. W. A reconnaissance study of herbicides and their metabilites in surface water of the midwestern United States using immunoassay and gas chromatography/mass spectrometry. *Environ. Sci. Technol.* **1992**, *26* (12), 2440−2447.

(4) Chiron, S.; Fernandez-Alba, A.; Rodriguez, A.; Garcia-Calvo, E. Pesticide chemical oxidation: state-of-the-art. *Water Res.* **2000**, *34* (2), 366−377.

(5) Watts, R. J.; Teel, A. L. Chemistry of modified Fenton's reagent (catalyzed H_2O_2 propagations−CHP) for in situ soil and groundwater remediation. *J. Environ. Eng.* **2005**, *131* (4), 612−622.

(6) Deguillaume, L.; Leriche, M.; Chaumerliac, N. Impact of radical versus non-radical pathway in the Fenton chemistry on the iron redox cycle in clouds. *Chemosphere* **2005**, *60*, 718−724.

(7) Huling, S. G.; Arnold, R. G.; Jones, P. K.; Sierka, R. A. Predicting Fenton-driven degradation using contaminant analog. *J. Environ. Eng.* **2000**, *126* (4), 348−353.

(8) Huling, S. G.; Arnold, R. G.; Sierka, R. A.; Miller, M. R. Measurement of hydroxyl radical activity in a soil slurry using the spin trap α-(4-pyridyl-1-oxide)-*N*-*tert*-butylnitrone. *Environ. Sci. Technol.* **1998**, *32*, 3436−3441.

(9) Paciolla, M. D.; Davies, G.; Jansen, S. A. Generation of hydroxyl radicals from metal-loaded humic acids. *Environ. Sci. Technol.* **1999**, *33* (11), 1814−1818.

(10) Watts, R. J.; Bottenberg, B. C.; Hess, T. F.; Jensen, M. D.; Teel, A. L. Role of reductants in the enhanced desorption and transformation of chloroaliphatic compounds by modified Fenton's reactions. *Environ. Sci. Technol.* **1999**, *33*, 3432−3437.

(11) Gallard, H.; Laat, J. D. Kinetic modelling of Fe(III)/H_2O_2 oxidation reactions in dilute aqueous soution using atrazine as a model organic compound. *Water Res.* **2000**, *34* (12), 3107−3116.

(12) Gallard, H.; Laat, J. D. Kinetics of oxidation of chlorobenzenes and phenyl-ureas by Fe(II)/H_2O_2 and Fe(III)/H_2O_2. Evidence of reduction and oxidation reactions of intermediates by Fe(II) or Fe(III). *Chemosphere* **2001**, *42* (4), 405−413.

(13) Weeks, K. R.; Bruell, C. J.; Mohanty, N. R. Use of Fenton's reagent for the degradatiion of TCE in aqueous systems and soil slurry. *Soil Sediment Contam.* **2000**, *9* (4), 331−345.

(14) Chen, G.; Hoag, G. E.; CHedda, P.; Nadim, F.; Woody, B. A.; Dobbs, G. M. The mechanism and applicability of in situ oxidation of trichloroethylene with Fenton's reagent. *J. Hazard. Mater.* **2001**, *87* (1−3), 171−186.

(15) Kanel, S. R.; Neppolian, B.; Choi, H.; Yang, J.-W. Heterogeneous catalytic oxidation of phenanthrene by hydrogen peroxide in soil slurry: Kinetics, mechanism, and implication. *Soil Sediment Contam.* **2003**, *12* (1), 101−117.

(16) Lin, S.-S.; Gurol, M. D. Catalytic decomposition of hydrogen peroxide on iron oxide: kinetics, mechanism, and implications. *Environ. Sci. Technol.* **1998**, *32* (10), 1417−1423.

(17) Watts, R. J.; Sarasa, J.; Loge, F. J.; Teel, A. L. Oxidative and reductive pathways in manganese-catalyzed Fenton's reactions. *J. Environ. Eng.* **2005**, *131* (1), 158−164.
(18) Lindsey, M. E.; Tarr, M. A. Inhibited hydroxyl radical degradation of aromatic hydrocarbons in the presence of dissolved fulvic acid. *Water Res.* **2000**, *34* (8), 2385−2389.
(19) Wang, Q.; Lemley, A. T. Kinetic effect of humic acid on alachlor degradation by anodic Fenton treatment. *J. Environ. Qual.* **2004**, *33*, 2343−2352.
(20) Pignatello, J. J.; Baehr, K. Ferric complexes as catalysts for "Fenton" degradation of 2,4-D and metolachlor in soil. *J. Environ. Qual.* **1994**, *23*, 365−370.
(21) Quan, H. N.; Teel, A. L.; Watts, R. J. Effect of contaminant hydrophobicity on hydrogen peroxide dosage requirements in the Fenton-like treatment of soils. *J. Hazard. Mater.* **2003**, *102* (2−3), 277−289.
(22) Paciolla, M. D.; Kolla, S.; Jansen, S. A. The reduction of dissolved iron species by humic acid and subsequent production of reactive oxygen species. *Adv. Environ. Res.* **2002**, *7*, 169−178.
(23) Vione, D.; Merlo, F.; Maurino, V.; Minero, C. Effect of humic acids on the Fenton degradation of phenol. *Environ. Chem. Lett* **2004**, *2*, 129−133.
(24) Watts, R. J.; Stanton, P. C.; Howsawkeng, J.; Teel, A. L. Mineralization of a sorbed polycyclic aromatic hydrocarbon in two soils using catalyzed hydrogen peroxide. *Water Res.* **2002**, *36* (17).
(25) Watts, R. J.; Udell, M. D.; Monen, R. M. Use of iron mineral in optimizing the peroxide treatment of contaminanted soils. *Water Environ. Res.* **1993**, *65*, 839−844.
(26) Watts, R. J.; Teel, A. L. Treatment of contaminated soils and groundwater using ISCO. *Pract. Period. Hazard., Toxic, Radioactive Waste Manage.* **2006**, *10*, 2−9.
(27) Wang, Q.; Lemely, A. T. Kinetic model and optimization of 2,4-D degradation by anodic Fentn treatment. *Environ. Sci. Technol.* **2001**, *35* (22), 4509−4514.
(28) Wang, Q.; Lemley, A. T. Oxidation of carbaryl in aqueous solution by membrane anodic Fenton treatment. *J. Agric. Food Chem.* **2002**, *50* (8), 2331−2337.
(29) Wang, Q.; Lemley, A. T. Competitive degradation and detoxification of carbamate insecticides by membrane anodic Fenton treatment. *J. Agric. Food Chem.* **2003**, *51* (18), 5382−5390.
(30) Wang, Q.; Scherer, E. M.; Lemley, A. T. Metribuzin degradaton by membrane anodic Fenton treatment and its interacton with ferric ion. *Environ. Sci. Technol.* **2003**, *38* (4), 1221−1227.
(31) Huckaba, C. E.; Keyes, F. G. The accuracy of estimation of hydrogen peroxide by potassium permanganate titration. *J. Am. Chem. Soc* **1948**, *70*, 1640.
(32) *SigmaPlot 9.0*, Systat Software Inc.
(33) MINITAB Statistic Software, 14, demo; Minitab Inc.
(34) Lindsey, M. E.; Tarr, M. A. Quantification of hydroxyle radical during Fenton oxidation following a single addition of iron and peroxide. *Chemsphere* **2000**, *41* (3), 409−417.
(35) Watts, R. J.; Udell, M. D.; Rauch, P. A. Treatment of pentachlorophenol-contaminated soils using Fenton's reagent.. *Hazard. Waste Hazard. Mater.* **1990**, *7*, 335−345.

Received for review January 5, 2006. Revised manuscript received March 24, 2006. Accepted March 28, 2006. This work is supported by the Cornell University Agricultural Experiment Station federal formula funds, Project 329423 (Regional Project W-045), received from CSREES, USDA.

JF060046X